

# Self-paced movement intention recognition from EEG signals during upper limb robot-assisted rehabilitation

Luis G. Hernández\* and Javier M. Antelis\*

**Abstract**—Currently, one of the challenges in EEG-based brain-computer interfaces (BCI) for neurorehabilitation is the recognition of the intention to perform different movements from same limb. This would allow finer control of neurorehabilitation and motor recovery devices by end-users [1]. To address this issue, we assess the feasibility of recognizing two self-paced movement intentions of the right upper limb plus a rest state from EEG signals recorded during robot-assisted rehabilitation therapy. In addition, the work proposes the use of Multi-CSP features and deep learning classifiers to recognize movement intentions of the same limb. The results showed performance peaked greater at (80%) using a novel classification models implemented in a multiclass classification scenario. On the basis of these results, the decoding of the movement intention could potentially be used to develop more natural and intuitive robot assisted neurorehabilitation therapies.

## I. INTRODUCTION

Electroencephalogram (EEG) based Brain-Computer Interfaces (BCI) for neurorehabilitation is a technology that provides the user with a non-muscular communication channel to trigger robot-assisted rehabilitation devices. Hence, an essential component in EEG-based BCIs is the experimental paradigm or mental task carried out by the user since this allows to induce recognizable patterns or changes in the recorded EEG signals. The most common paradigm in BCI is motor imagery (MI). Here, the user imagines the movement of different body limbs which is recognized within a bi-class classification scenario (e.g., left hand MI versus right hand MI) from features extracted from the recorded EEG signals. To do so, the user is guided with visual or auditory cues to initiate and to end the movement imagery (i.e., synchronous BCI), afterwards the EEG is analyzed and classified to send a control signal to the external device.

Although EEG-based BCIs with MI paradigm are used in neurorehabilitation with satisfactory results there are still unsolved needs in order to promote rehabilitation and recovery at both the physical and brain cortical levels. For example, to promote neural reorganization it is necessary that the robot-assisted rehabilitation robots execute the movements while the user is also performing the mental task. This is not the case is a classical BCI with MI because there is a inherent delay between movement imagination carried out by the user and the physical output of the robot-assisted rehabilitation devices. Furthermore, the success of a neurorehabilitation with a BCI requires a match between the mental task performed by the user and the movements performed by the robotic devices. Again, this is not the case

with the MI paradigm since the user usually imagines body movements that are easy to recognize but that are not the same as the movements performed by the robots. Finally, BCI driven rehabilitation therapies for a single limb, as those required for survivors affected by unilateral stroke, requires the recognition of diverse movements of the same limb to produce different movements in the robot-assisted rehabilitation devices. This is however a challenging task when using EEG signals because the same brain region is involved in the planning and execution of the those movements, and thus, the recognition is more difficult. For these reasons, BCI for neurorehabilitation, especially of the same limb, requires the anticipatory recognition of natural and several movements from the EEG activity, i.e., the recognition of the "intention" of "several movements" in the same limb. Recent studies have proposed decoding upper limb information from EEG signals [2], [3], [4]. Nevertheless, it is necessary to extend these investigations to the anticipatory detection of several self-initiated and self-selected movements of the same limb with robot-assisted rehabilitation devices.

This work studied these issues in an experimental task with seven healthy participants and a motor rehabilitation device for the upper limb. The experiment consisted of two self-initiated and self-selected movements of the right upper limb while the EEG signal are recorded. The aim is to assess the recognition of the two movement intention from EEG signals. In addition, this work also explores the use of novel classification models based on deep learning to address the classification of multiple classes, i.e., the two movement intention of the same limb plus a rest state. This is important because the conventional way to classify EEG signals into several classes employs multiclass-extended strategies (a voting scheme that combine the decisions of several classifiers for a more accurate output) of bi-class classifiers such as support vector machines (SVM) [5] and the use of a single classification model might enhance classification accuracy which could be significant for the development of online BCI applications for neurorehabilitation or other applications.

In particular, we used convolutional neural networks (CNN) and recurrent neural network (RNN) and compare there performance with SVM to recognize the two movement intention and a rest state from EEG signals. The analysis of the EEG activity showed a significant event-related desynchronization in the motor-related frequency bands of the EEG that precedes the movement initiation. This suggests the existence of neural correlates useful for recognizing movement intention. The three-class classification results, on the other hand, showed a classification accuracy averaged

\*School of Engineering and Science, Tecnológico de Monterrey en Guadalajara, Jalisco, Mexico, [www.tec.mx](http://www.tec.mx)

across-all-participant of  $0.65 \pm 0.09$ ,  $0.68 \pm 0.15$   $0.65 \pm 0.11$  for SVM, CNN and RNN, respectively. This indicates that it is possible to recognize the intention to performs two different movements of the same upper limb and the rest state and that its is feasible to use deep leaning based classifiers to accomplish this task.

## II. MATERIALS AND METHODS

### A. Data recording

Seven healthy subjects participated in this study. The experiment was conducted in accordance to the Helsinki declaration. All participants were duly informed about the goals of the research. The experimental task consisted of self-selected and self-initiated movements of the right arm using a neurorehabilitation device Tee-R on passive mode [6]. The movements were (A) supination/pronation of the forearm (Fig.1a) and (B) flexion/extension of the arm (Fig.1b). During the execution of the experiment, EEG signals were recorded from 62 scalp locations according to the international 10/20 system using a g.HIamp amplifier (g.tec medical engineering GmbH, Austria). The reference and ground electrode were placed over left earlobe and AFZ, respectively. The EEG signals were acquired at a sampling frequency of 1200 Hz and no filtering was applied. In addition, two digital signals from Tee-R were also recorded which indicated the movement type and the movement onset.

### B. Experimental Design

The experiment consisted of many trials which was controlled by three visual cues (See Fig.1c). The subject is first shown for three seconds an image with the text "Relax" with the robot in the home position. The subject is then shown for 12 seconds an image with a cross and indicating to perform any of two movements (self-selected). Also, they were asked to initiate the movement whenever they desired (waiting around 6 seconds after the cross was first displayed while avoiding any mental count). This means that they decided when to initiate the movement (self-initiated). Finally, the subject is shown for 3 seconds an image with the text "rest" indicating rest, move or blink. Altogether, 120 trials were recorded per subject, 60 trials of each movement type.

### C. Data Pre-processing

EEG signals were low-pass filtered at a cutoff frequency of 50 Hz using a 2nd-order zero-phase shift Chebychev-type filter and a common average referenced (CAR) filter was also applied. Subsequently, visual artifact rejection was applied to rule out noise-contaminated trials. Afterwards, EEG signals were trimmed to 15 seconds long trials starting from the first visual cue and up to the second visual cue. Then, the zero time reference was aligned with movement onset signals obtained from the Tee-R. Therefore, all trials have the same reference at the movement initiation ( $t = 0$ ) but different trials initiation ( $t_{ini}$ ) and trial end ( $t_{end}$ ). According to this, the time segment  $[t_{ini}, t_{ini}+3]$ s and  $[-3, 0]$ s correspond to relax and movement intention, respectively. Finally, the time segments of all the trials were labelled according to the motor stage (i.e., *Relax*, *Int A*, *Int B*) to construct the EEG dataset.

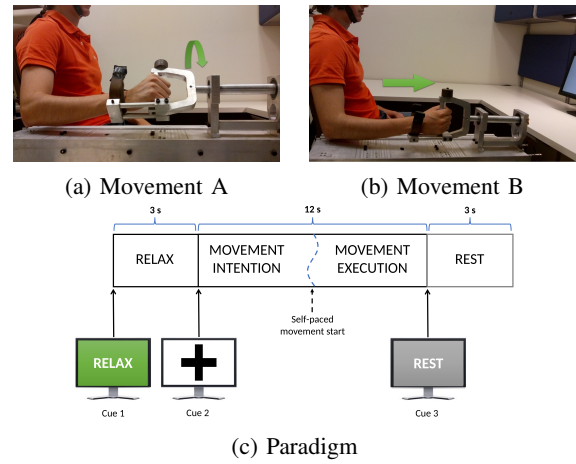


Fig. 1. Illustration of the two movements: (a) movement A (supination/pronation of the forearm); (b) movement B flexion/extension of the arm). (c) Description of the experimental paradigm for self-selected and self-initiated movements

### D. Event-related desynchronization/synchronization

To understand the task-related oscillatory EEG signals the event related desynchronization/synchronization (ERD/ERS) was computed for each electrode following [7] at the significant level of  $\alpha = 0.05$ . This analysis shows the dynamic evolution of energy during the execution of the task. This analysis is relevant because oscillations in the alpha and beta bands can display either an event-related blocking response [8] which can be associated to motion planning processes. A bootstrap analysis of the time-frequency representation was calculated in the frequency band  $[4 - 45]$ Hz at the resolution of 1Hz using Morlet wavelets. The trials were trimmed from  $-2.5$  to 1s allowing all trials to have the same length. The energy changes relative to the baseline  $[-2.5, -1.5]$ s was computed for each time and frequency.

### E. Detection of Movement Intention

1) *Features*: The features were extracted through the Common Spatial Pattern (CSP) algorithm which is a technique commonly used in bi-class classification scenarios in MI tasks. This is because the goal of CSP is to find a set of spatial filters that maximize the variance of signals between two conditions. CSP algorithm has been extended to a multiclass approach. In this work we use the One-Versus-the-Rest (OVR) algorithm which is a multiclass extension of CSP algorithm [9]. CSP features corresponding to *Relax* state were extracted from the interval  $[t_{ini} + 2, t_{ini}+1]$ s and CSP features corresponding to *Int A* and *Int B* states were extracted from  $[t_{ini} + 2, t_{ini}+1]$ s CSP filters were designed for the frequency window 7-30 Hz and the log-variance of the CSP-filtered signals were used as features. The application of this multiclass CSP resulted a feature vector of 1116 (used as input for SVM) or equivalently is the feature map of  $62 \times 18$  (used as input for CNN and RNN). The number of spatial filters and the number of features were selected in accordance to prior studies with CSP features [10], [3].

2) *Classifiers*: In this research, 3 classifiers architectures were implemented and assessed to discriminate between *Relax*, *Int A* and *Int B* from EEG signals: *i*) Support vector machine with Radial Basis function kernel (SVM) and hyperparameters  $C = 1.0$  and  $\gamma = 0.01$ . In this classifier an one-versus-one strategy (which yields to 3 binary classifiers) was employed to address the multi-class classification; *ii*) Convolutional neural network (CNN). The CNN architecture employed is described in [11], [12]; and *iii*) Recurrent Neural network. The RNN architecture consisted of 62 timesteps with input size 18 and 128 hidden units. All of them were implemented with Tensorflow Library [13] and executed in a Geforce GTX Titan Xp GPU (Nvidia,USA).

3) *Performance Evaluation*: Classification accuracy was assessed independently for each participant. The total dataset was randomly splitted into two mutually exclusive sets. The training set consisted of 80% of the data while the evaluation set consisted of the rest 20% of the data. The algorithms were trained in 400 steps. At each step, a batch of training data (20% of the training set) is sampled randomly and used to feed the classification model. Performance metric was classification accuracy which was computed as:

$$accuracy = \frac{TP + TN}{TP + TN + FP + FN} \quad (1)$$

where  $TP$  is the true positive rate,  $TN$  is the true negative rate,  $FP$  is the false positive rate and  $FN$  is the false negative rate. The performance evaluation is repeated 10 times and the distribution and *mean*  $\pm$  *std* of the classification accuracy were computed. The significant classification accuracy chance level was considered as  $accuracy_{chance} = 33.33\%$ .

### III. RESULTS

The movement type and the time instant of the movement onset computed with the Tee-R activity was estimated in all the trials for all subjects. The movement onset was lower than 1s in 2% of the trials while it was greater than 9s in 1% of the trials. These trials were discharged and not used in the rest of the work. Table I shows a summary of the movement onset for all subjects and the average for all of them. The average movement onset across all subjects was  $5.32 \pm 1.76s$  (minimum of 1.16s and a maximum 9.54s). The event-related desynchronization/synchronization analysis was performed for each subject independently. Fig. 2 shows these results for one of the participants in electrodes C1 and C2. Significant desynchronization ( $p < 0.05$ ) is observed in the two electrodes and in the motor-related  $\alpha[8,13]Hz$  and  $\beta[14,30]Hz$  frequency bands around the zero-time. However, the desynchronization is more intense in electrode C1 than in electrode C2, which is congruent with the motor task where the participant moved the right upper limb. This significant desynchronization starts in the movement intention phase roughly at 0.7s prior to the movement onset and remains significant up to the movement execution interval. No significant desynchronization or synchronization is observed before  $-1.0s$ .

The distribution of classification accuracy was obtained with the three classification models for each participant. For

TABLE I  
SUMMARY OF MOVEMENT ONSET TIME FOR EACH PARTICIPANT ( $P_1$  TO  $P_7$ ) FOR THE TWO EXPERIMENTAL MOVEMENTS

Participant	Movement	Mean	$\pm$ SD	Max	Min
$P_1$	Mov A	4.31	0.54	6.24	3.54
	Mov B	4.62	0.85	7.34	3.50
	Both	4.47	0.73	7.34	3.50
$P_2$	Mov A	4.79	0.60	6.47	3.50
	Mov B	4.81	0.65	6.25	3.55
	Both	4.80	0.62	6.47	3.50
$P_3$	Mov A	6.66	0.89	8.77	3.60
	Mov B	6.90	0.73	8.44	4.84
	Both	6.78	0.82	8.77	3.60
$P_4$	Mov A	5.61	1.10	8.63	2.60
	Mov B	5.79	1.15	8.66	2.14
	Both	5.71	1.13	8.66	2.14
$P_5$	Mov A	5.30	2.01	8.58	1.67
	Mov B	5.85	1.92	8.72	1.74
	Both	5.57	1.97	8.72	1.67
$P_6$	Mov A	4.99	1.26	8.11	1.75
	Mov B	4.76	1.28	7.15	1.74
	Both	4.87	1.27	8.11	1.74
$P_7$	Mov A	4.96	1.95	8.00	1.63
	Mov B	7.22	1.83	9.54	1.93
	Both	5.08	1.89	9.54	1.63
Avg	Mov A	5.21	1.94	8.77	1.63
	Mov B	5.70	1.58	9.54	1.74
	Both	5.32	1.76	9.54	1.63

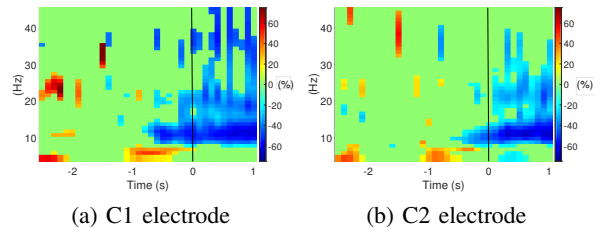


Fig. 2. Significant event-related desynchronization/synchronization activity computed for participant 1 in C1 and C2 electrodes. Horizontal axis represents time (units of s) while vertical axis represents frequency (units of Hz), colorbar represents percentage value of changes. Significant desynchronization ( $p < 0.05$ ) is observed in the motor-related  $\alpha[8,13]Hz$  and  $\beta[14,30]Hz$  frequency bands from 1.0s, while no significant desynchronization or synchronization is observed before 1.0s

all participants and in the three classifiers, the median of the distributions were higher and significantly different than the chance level of 33% ( $p < 0.05$ ). To examine differences across participants and classification models, Table II summarizes the classification results and shows the average across all participants. The classification accuracy is greater with the SVM in participant 2 ( $0.70 \pm 0.04$ ), with the CNN in participants 1, 4 and 6 ( $0.73 \pm 0.13$ ,  $0.72 \pm 0.04$  and  $0.68 \pm 0.02$ , respectively) and with the RNN in participants 3, 5 and 7 ( $0.64 \pm 0.05$ ,  $0.70 \pm 0.05$  and  $0.67 \pm 0.04$ , respectively). Likewise, the average classification accuracy was  $0.65 \pm 0.09$ ,  $0.68 \pm 0.15$  and  $0.65 \pm 0.11$  for SVM, CNN and RNN, respectively. This shows that, on average, CNN provides the highest classification rates though the accuracy provided by this classifier is only 3% greater than the accuracy achieved with SVM and CNN.

TABLE II

SUMMARY OF CLASSIFICATION ACCURACY RESULTS FOR EACH PARTICIPANT ( $P_1$  TO  $P_7$ ) ACHIEVED WITH THE SVM, CNN AND RNN.

Participant	Model	Mean	SD	Max	Min
$P_1$	SVM	0.65	0.03	0.74	0.63
	CNN	0.73	0.13	0.85	0.59
	RNN	0.67	0.08	0.75	0.60
$P_2$	SVM	0.70	0.04	0.80	0.62
	CNN	0.68	0.06	0.79	0.57
	RNN	0.65	0.11	0.79	0.37
$P_3$	SVM	0.62	0.02	0.67	0.59
	CNN	0.60	0.05	0.69	0.50
	RNN	0.64	0.05	0.71	0.58
$P_4$	SVM	0.70	0.04	0.76	0.64
	CNN	0.72	0.04	0.69	0.58
	RNN	0.59	0.05	0.67	0.53
$P_5$	SVM	0.67	0.03	0.70	0.59
	CNN	0.68	0.09	0.81	0.51
	RNN	0.70	0.05	0.77	0.60
$P_6$	SVM	0.61	0.02	0.64	0.57
	CNN	0.68	0.02	0.71	0.64
	RNN	0.66	0.02	0.70	0.62
$P_7$	SVM	0.62	0.03	0.72	0.58
	CNN	0.65	0.05	0.74	0.59
	RNN	0.67	0.04	0.74	0.61
Avg	SVM	0.65	0.09	0.80	0.57
	CNN	0.68	0.15	0.85	0.50
	RNN	0.65	0.11	0.79	0.37

#### IV. CONCLUSION

This work studied the recognition of several movement intention of the same limb using EEG signals recorded during a self-selected and self-initiated motor task. In addition, the work assessed the performance of convolutional and recurrent neural networks to recognize three motor stages, i.e., a three-class classification scenario. For that, EEG signals from seven healthy participants were recorded during an upper limb movement task assisted by a robotic rehabilitation device. The event-related desynchronization/synchronization analysis of the EEG activity revealed significant power decrease in the motor-related frequency bands that initiated roughly 0.7s prior to the movement onset. This indicates the existence of neural correlates during movement planning associated to the motor task, which can be used as features to recognize movement intention.

To recognize between *Relax*, *Supination/pronation intention* and *Flexion/extension intention*, multiclass common spatial patterns were used to extract features while support vector machine (SVM), convolutional neural network (CNN) and recurrent neural network (RNN) were used as classification algorithms. The classification accuracy results were on average  $0.65 \pm 0.09$ ,  $0.68 \pm 0.15$  and  $0.65 \pm 0.11$  for SVM, CNN and RNN, respectively, which showed that the CNN and RNN techniques can be used for decoding movement intention from EEG signals under a neurorehabilitation therapy. These results cannot be compared with the state of the art due to there are several differences with those works [2], [3], [4], for instance, the experimental setup (e.g., execution of different movements), the conditions of the participants (e.g., patients with motor injury), and the difference of the EEG attributes used for classification (e.g., temporal features). The

results presented herein showed the feasibility to recognize intention of movement in different movements of the same upper limb. The detection of the intention to move a limb and the recognition of the type of movement is essential to properly trigger robot-assisted rehabilitation robots. This is a critical characteristic of BCI for neurorehabilitation that aim to recovery physical functions but also the neural reorganization since the user will attain fast and natural brain control during the rehabilitation therapy. However, it is still necessary to extend the numbers of subjects to achieve significant statistics and to carry out further study to validate this movement intention decoding in on-line settings with real end-users.

#### ACKNOWLEDGMENT

This work is supported by the National Council of Science and Technology of Mexico (CONACyT) through grants 268958 and PN2015-873.

#### REFERENCES

- [1] S. R. Soekadar, N. Birbaumer, M. W. Slutzky, and L. G. Cohen, "Brain machine interfaces in neurorehabilitation of stroke," *Neurobiology of Disease*, vol. 83, pp. 172–179, 2015.
- [2] P. Ofner, A. Schwarz, J. Pereira, and G. R. Müller-Putz, "Upper limb movements can be decoded from the time-domain of low-frequency EEG," *PLoS One*, vol. 12, no. 8, p. e0182578, Aug 2017, pONE-D-17-04785[PII].
- [3] F. Shiman, E. López-Larraz, A. Sarasola-Sanz, N. Irastorza-Landa, M. Spler, N. Birbaumer, and A. Ramos-Murguialday, "Classification of different reaching movements from the same limb using EEG," *Journal of Neural Engineering*, vol. 14, no. 4, p. 046018, 2017.
- [4] J. Pereira, A. I. Sburlea, and G. R. Müller-Putz, "EEG patterns of self-paced movement imaginations towards externally-cued and internally-selected targets," *Scientific Reports*, vol. 8, no. 1, p. 13394, 2018.
- [5] R. Vega, T. Sajed, K. W. Mathewson, K. Khare, P. M. Pilarski, R. Greiner, G. Sánchez-Ante, and J. M. Antelis, "Assessment of feature selection and classification methods for recognizing motor imagery tasks from electroencephalographic signals," *Artif. Intell. Research*, vol. 6, no. 1, p. 37, 2017.
- [6] I. Figueroa-García *et al.*, "Platform for the study of virtual task-oriented motion and its evaluation by EEG and EMG biopotentials," in *2014 36th Annual International Conference of the IEEE Engineering in Medicine and Biology Society*, Aug 2014, pp. 1174–1177.
- [7] B. Graimann and G. Pfurtscheller, "Quantification and visualization of event-related changes in oscillatory brain activity in the time-frequency domain," in *Event-Related Dynamics of Brain Oscillations*, ser. Progress in Brain Research, C. Neuper and W. Klimesch, Eds. Elsevier, 2006, vol. 159, pp. 79 – 97.
- [8] G. Pfurtscheller and F. L. da Silva, "Event-related EEG/MEG synchronization and desynchronization: basic principles," *Clinical Neurophysiology*, vol. 110, no. 11, pp. 1842 – 1857, 1999.
- [9] G. Dornhege, B. Blankertz, G. Curio, and K. Müller, "Boosting bit rates in noninvasive EEG single-trial classifications by feature combination and multiclass paradigms," *IEEE Transactions on Biomedical Engineering*, vol. 51, no. 6, pp. 993–1002, 2004.
- [10] X. Yong and C. Menon, "EEG classification of different imaginary movements within the same limb," *PLOS ONE*, vol. 10, no. 4, pp. 1–24, 04 2015.
- [11] L. G. Hernández, O. M. Mozos, J. M. Ferrández, and J. M. Antelis, "EEG-based detection of braking intention under different car driving conditions," *Frontiers in Neuroinformatics*, vol. 12, p. 29, 2018. [Online]. Available: <https://www.frontiersin.org/article/10.3389/fninf.2018.00029>
- [12] L. G. Hernández and J. M. Antelis, "A comparison of deep neural network algorithms for recognition of EEG motor imagery signals," in *Pattern Recognition*, 2018, pp. 126–134.
- [13] M. Abadi *et al.*, "TensorFlow: Large-scale machine learning on heterogeneous systems," 2015, software available from tensorflow.org. [Online]. Available: <https://www.tensorflow.org/>